

Giant lattice softening at a Lifshitz transition in Sr_2RuO_4

H. M. L. Noad^{1*}, K. Ishida^{1†}, Y.-S. Li¹, E. Gati¹, V. Stangier², N. Kikugawa³, D. A. Sokolov¹, M. Nicklas¹, B. Kim^{4,5}, I. I. Mazin^{6,7}, M. Garst^{8,9}, J. Schmalian^{2,9*}, A. P. Mackenzie^{1,10*}, C. W. Hicks^{1,11*}

The interplay of electronic and structural degrees of freedom in solids is a topic of intense research. More than 60 years ago, Lifshitz discussed a counterintuitive possibility: lattice softening driven by conduction electrons at topological Fermi surface transitions. The effect that he predicted, however, was small and has not been convincingly observed. Using a piezo-based uniaxial pressure cell to tune the ultraclean metal strontium ruthenate while measuring the stress-strain relationship, we reveal a huge softening of the Young's modulus at a Lifshitz transition of a two-dimensional Fermi surface and show that it is indeed driven entirely by the conduction electrons of the relevant energy band.

The coupling between elastic and electronic degrees of freedom is crucial to determining the phase diagrams of correlated electron systems, such as those displaying electronic nematicity, in which conduction electrons develop anisotropies (1). However, there is always a “chicken and egg” question: Does the lattice drive or respond to the conduction electron physics (2, 3)? Here, we approached the entanglement of electronic and structural degrees of freedom using a different method from those most commonly used. We studied the stress-strain relationship of the quasi-two-dimensional (2D) correlated metal strontium ruthenate (Sr_2RuO_4) as it was tuned through a saddle point Lifshitz transition (4–6) in which the Fermi surface topology changes and the Fermi level crosses a Van Hove singularity (VHS) (7). By combining direct stress-strain measurements with experimentally determined entropy data across the same transition, we have demonstrated the existence of an unexpectedly large softening of the lattice driven entirely by conduction electrons. The possibility of such effects was discussed theoretically by Lifshitz him-

self >60 years ago, but their size was estimated to be extremely small (4). By contrast, here, we measured a large effect that is in principle singular, i.e., capable of introducing a lattice instability in the $T \rightarrow 0$ limit if not cut off by a phase transition to some other form of order. We discuss our results in the framework of quantum critical elasticity and show that superconductivity is a natural way of cutting off quantum critical lattice softening.

Young's modulus dips across a stress-tuned Lifshitz transition in Sr_2RuO_4

The material platform for our experiments, Sr_2RuO_4 , has attracted considerable attention both as an unconventional superconductor (8–12) and as a benchmark 2D Fermi liquid (13, 14). It is one of the cleanest correlated electron materials known. The best single crystals have residual resistivities of ≈ 50 n Ω cm, corresponding to electron mean free paths of 2 μm or more (15). The Fermi surface of Sr_2RuO_4 consists of three cylinders, commonly referred to as α , β , and γ (14). Electronic correlations lead to a substantial mass renormalization over the values predicted in independent-electron band

structure calculations, meaning that unambiguously, the Fermi energy (E_F) of the γ band sits only 14 meV below a saddle point VHS at the M point of the tetragonal Brillouin zone (16). It is possible to tune this VHS through E_F by applying a pressure of 0.7 ± 0.1 GPa along the [100] crystalline direction (17, 18), profoundly affecting the electronic properties. For example, the superconducting transition temperature is enhanced by a factor of 2.4 from its ambient pressure value to 3.5 K (19), and the temperature dependence of the resistivity undergoes a large change from the conventional Fermi liquid T^2 dependence seen at higher and lower stress (5).

To investigate the consequences of this Lifshitz transition on the lattice stiffness, we used a custom apparatus in which both uniaxial stress σ and strain ε can be monitored simultaneously (20), allowing measurement of the Young's modulus (fig. S1). To maximize the quantitative accuracy of the data, samples were milled into a necked shape, as shown in the inset of Fig. 1A, using a Xe plasma source focused ion beam. The end tabs were then

¹Max Planck Institute for Chemical Physics of Solids, 01187 Dresden, Germany. ²Institut für Theorie der Kondensierten Materie, Karlsruher Institut für Technologie, 76131 Karlsruhe, Germany. ³National Institute for Materials Science, Tsukuba, Ibaraki 305-0003, Japan. ⁴Department of Physics, Kunsan National University, Gunsan 54150, Korea. ⁵Department of Physics, Kyungpook National University, Daegu 41566, Korea. ⁶Department of Physics and Astronomy, George Mason University, Fairfax, VA 22030, USA. ⁷Quantum Science and Engineering Center, George Mason University, Fairfax, VA 22030, USA. ⁸Institut für Theoretische Festkörperphysik, Karlsruher Institut für Technologie, 76131 Karlsruhe, Germany. ⁹Institut für QuantenMaterialien und Technologien, Karlsruher Institut für Technologie, 76131 Karlsruhe, Germany. ¹⁰Scottish Universities Physics Alliance, School of Physics and Astronomy, University of St Andrews, St Andrews KY16 9SS, UK. ¹¹School of Physics and Astronomy, University of Birmingham, Birmingham B15 2TT, UK. *Corresponding author. Email: hiliary.noad@cphys.mpg.de (H.M.L.N.); joerg.schmalian@kit.edu (J.S.); andy.mackenzie@cphys.mpg.de (A.P.M.); c.hicks.1@bham.ac.uk (C.W.H.) †Present address: Institute for Materials Research, Tohoku University, Sendai 980 8577, Japan.

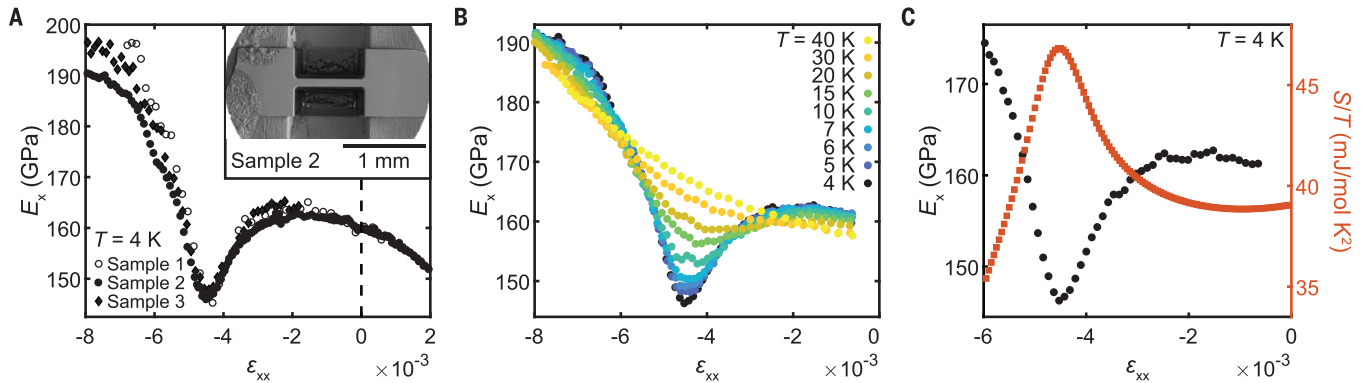


Fig. 1. The Young's modulus E_x of Sr_2RuO_4 measured across a stress-tuned Lifshitz transition. (A) E_x as a function of strain ε_{xx} measured at 4 K on three samples. Inset: Scanning electron micrograph of sample 2. (B) E_x versus ε_{xx} at a series of temperatures measured on sample 2. (C) E_x at 4 K taken from the temperature series in (B) (black) together with the entropy S/T extracted from elastocaloric data from a separate sample at 4 K (orange) plotted as a function of ε_{xx} . The elastocaloric data are from (23).

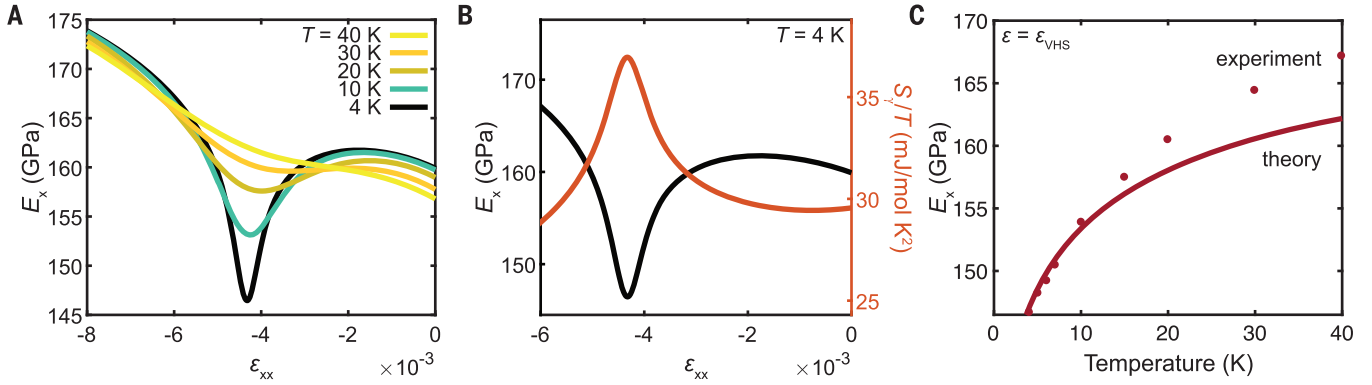


Fig. 2 A simple model quantitatively reproduces key experimental features. (A) Calculated E_x versus ϵ_{xx} at selected temperatures. (B) E_x and S_γ/T versus ϵ_{xx} at 4 K, where S_γ is the calculated contribution to the entropy of the γ band. (C) E_x versus temperature calculated at the Van Hove strain (solid line) and corresponding experimental data (filled circles) extracted from the temperature series shown in Fig. 1B. The averaging window for the data is a strain range of 3×10^{-4} . For details on the model, see (22).

embedded in epoxy, which acts as a conformal layer through which large forces can be transmitted to the brittle samples. The necking creates a rapid crossover between low- and high-stress regions of the sample, which is important for resolving fine features in the stress-strain relationship (21). Full details on how we extracted the Young's modulus and strain of the sample, including an examination of possible systematic errors that could affect the analysis, can be found in (22) and in figs. S2 to S5.

Our core result is shown in Fig. 1A: the differential Young's modulus $E_x = d\sigma_{xx}/d\epsilon_{xx}$ as a function of strain at 4 K. To demonstrate repeatability, data from three samples are shown. Samples 2 and 3 had a higher aspect ratio (22) and are therefore expected to yield more accurate data. Each sample was in a different stress cell. The force calibrations of the cells were refined using the known Lifshitz stress of -0.7 GPa (18), where negative values denote compression. At the Lifshitz transition strain of $\epsilon_{VHS} = -(0.45 \pm 0.05)\%$, E_x is seen to drop to ~ 146 GPa, and then beyond the transition to increase to ~ 200 GPa. In other words, contrary to our naive expectation, the dip in E_x is not a small effect; the softening of the lattice at the Lifshitz transition is between 10 and 15% depending on the definition used for the background value. Under tensile strain, E_x again decreases quite rapidly. A Lifshitz transition under tensile strain equivalent to that under compressive strain would be expected, and this decrease in E_x is most likely caused by the approach to that transition. A second notable aspect of the lattice softening at the Lifshitz strain is its strong temperature dependence, shown in Fig. 1B. At 40 K, the dip is barely resolved. As the temperature is lowered, it sharpens and deepens, with a substantial change observable even between 5 and 4 K.

Elastic constants are second derivatives of the free energy, $C = \frac{\partial^2 F}{\partial \epsilon^2}$, $F = U - TS$, where U is the internal energy and S is entropy. The intu-

itive expectation might be that the valence band contributions to U completely dominate F and thus also the elastic moduli. However, the generally valid expression for the free energy $F(T, \epsilon) = E_0(\epsilon) - \int_0^T S(T', \epsilon) dT'$, where E_0 is the ground state energy, reveals that any temperature dependence of elastic constants derives from changes in the entropy even if $E_0(\epsilon)$ may dominate the elastic moduli. Our Young's modulus data have a strong temperature dependence (Fig. 1B), so a link between the Young's modulus and a strain-dependent entropy would be expected. In Fig. 1C, we compare the entropy obtained from a recent study of the elastocaloric effect on Sr_2RuO_4 (23) at 4 K with the Young's modulus data at the same temperature. The strong correlation between the two leads to the conclusion that the key physics that we observe are driven by a conduction band. At this low temperature, the phonon contribution to the entropy in Sr_2RuO_4 is negligible (24) and the valence band contribution even more so. All that would be observed is conduction band entropy because of the density of states at the Fermi level.

Modeling lattice softening

To understand the observed behavior quantitatively, we made use of a 2D model for the Landau quasiparticles of the γ band (23), the parameters of which are all constrained by other observations on Sr_2RuO_4 (25). This model (22) yields a contribution $F_\gamma(T, \epsilon_{xx}, \epsilon_{yy}, \epsilon_{zz})$ to the electronic free energy as function of temperature and the three uniaxial strain values. The crucial ingredient of the theory is a symmetry-adapted deformation potential $\alpha \sim t^1 \partial t / \partial \epsilon$ with tight-binding hopping parameters t . (Notice that although we mostly refer to the uniaxial strain along the x axis as ϵ , we briefly write out the axis labels explicitly to account for the correct Poisson effects that enter any measurement of the Young's modulus.) The total free energy is then given as $F =$

$F_0 + F_\gamma$, where we determined F_0 such that our model reproduces the correct elastic constants for the unstrained samples at the reference temperature of $T = 4$ K. We included the applied uniaxial stress using $F \rightarrow F - \epsilon_{xx} \sigma_{xx}$ which yields the equation of state $\sigma_{xx} = \partial F / \partial \epsilon_{xx}$. In linear elasticity, strain orthogonal to the applied stress is accounted for by Poisson ratios, such as $\epsilon_{\kappa\kappa} = -\nu_{\kappa x} \epsilon_{xx}$ with $\kappa = y, z$. For the rather large stress values applied here and given the subtle behavior near the Lifshitz transition, we must, however, allow for nonlinear relations $\epsilon_{\kappa\kappa} = \epsilon_{\kappa\kappa}(\epsilon_{xx})$. Those follow from $\partial F / \partial \epsilon_{yy} = \partial F / \partial \epsilon_{zz} = 0$. This finally yields the differential Young's modulus

$$E_x = \frac{d\sigma_{xx}}{d\epsilon_{xx}} = C_{11} + C_{12} \frac{\partial \epsilon_{yy}(\epsilon_{xx})}{\partial \epsilon_{xx}} + C_{13} \frac{\partial \epsilon_{zz}(\epsilon_{xx})}{\partial \epsilon_{xx}} \quad (1)$$

with the usual definition of the elastic tensor. The elastic constants $C_{ij} = C_{0,ij} - \frac{2}{k_B T} \int \frac{d^3 k}{(2\pi)^3} f_{\mathbf{k}} \times (1 - f_{\mathbf{k}}) \frac{\partial E_{\mathbf{k}}}{\partial \epsilon_{ii}} \frac{\partial E_{\mathbf{k}}}{\partial \epsilon_{ij}}$ consist of a background contribution $C_{0,ij}$ and the part due to the γ band with strain-dependent $E_{\mathbf{k}}$ and Fermi function $f_{\mathbf{k}}$. Within linear elasticity, the derivatives are the strain-independent Poisson ratios and $1/E_x$ is the $i = j = 1$ element of the inverse of the elastic tensor C_{ij} in Voigt notation. We show in (22) that, near the Lifshitz point, $-\epsilon_{yy}/\epsilon_{xx}$ and the differential Poisson ratio $-\partial \epsilon_{yy} / \partial \epsilon_{xx}$ differ and have a pronounced strain dependence (fig. S6). Once these nonlinear Poisson's ratios were included, our model made the predictions shown in Fig. 2, A and B. The agreement with the experimental data shown in Fig. 1 is very good (see also fig. S7). The temperature dependence of the dip in the Young's modulus and the relationship between the Young's modulus and entropy at 4 K are reproduced well and provide evidence that the model correctly captures the key physics of the observations.

Qualitatively, the softening at the Van Hove point is a consequence of the fact that Young's modulus is the sum of a presumed weakly temperature- and strain-dependent background contribution, $E_x^{(0)}$, and a singular conduction electron contribution from the γ band

$$E_x \cong E_x^{(0)} - A \log \frac{1}{(T/T_0)^2 + (\epsilon_{xx} - \epsilon_{VHS})^2} \quad (2)$$

where A is a positive constant and T_0 is a temperature such that $k_B T_0$ is of the order of the electronic bandwidth. The logarithmic T and strain dependence stems from the fact that the electronic contribution to the elastic constants is proportional to the density of states [see the $f_k(1-f_k)$ term in the γ -band contribution to C_{ij}], which diverges logarithmically at a VHS in 2D. All electronic contributions to the C_{ij} and the differential Poisson's ratios also show this singular, logarithmic dependence. The sign of the coefficient $A > 0$ reflects that the γ band will always cause a softening of the important diagonal elements C_{ii} of the elastic tensor. The magnitude of A is determined by a combination of band renormalization factors and the deformation potential: $A \propto \alpha^2$.

A further prediction of the model is that the temperature dependence of the Young's modulus at the Lifshitz pressure has negative curvature, and this is indeed observed in our measurements (Fig. 2C). This negative curvature, in addition to the strong link between elastic and electronic degrees of freedom that our data have established, imply that the Young's modulus is related to an electronic susceptibility. The logarithmic softening, however, cannot continue down to the lowest temperatures. This interruption might be a consequence of a first-order structural transition, which was initially proposed by Lifshitz, or the formation of some electronic order that prevents a mechanical instability. One way in which the logarithm will be cut off in a quasi-2D material is by coherent 3D effects caused by interlayer hopping. However, in the highly 2D γ band of Sr_2RuO_4 , the scale for such processes is < 3 K (8). Whether the onset of superconductivity at $T_c = 3.5$ K is related to the mechanical stability of Sr_2RuO_4 is therefore an exciting open question.

Interplay with superconductivity

In this context, it was interesting to extend our Young's modulus measurements to the superconducting state in which a small gap is opened at the Fermi energy. As shown in Fig. 3, A and B, the strong normal-state softening of the lattice is indeed cut off by the onset of the superconductivity, with the lattice hardening again slightly below the superconducting T_c , an effect that is most pronounced at the Van Hove strain. By contrast, if we suppress the superconductivity by applying a 2 T out-of-plane

magnetic field, then the softening continues down to the lowest temperatures used in the measurement.

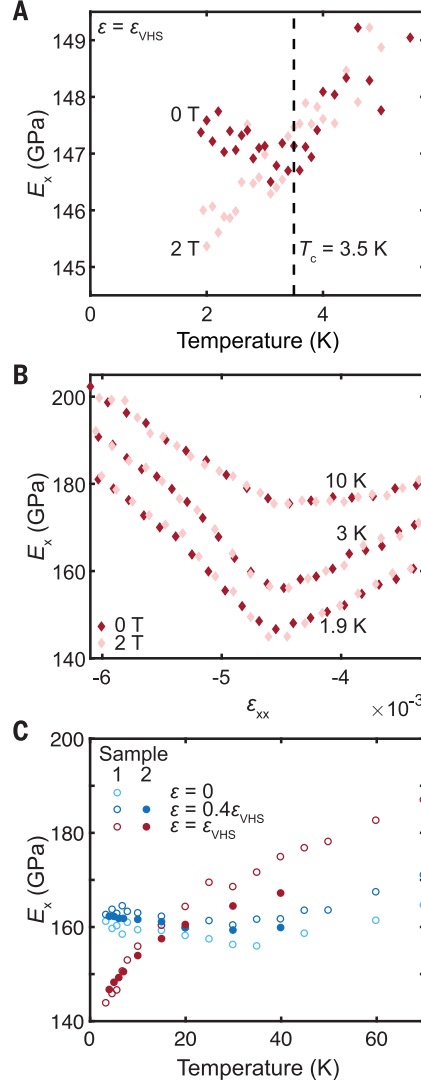


Fig. 3. Tracking E_x at key strains to lower and higher temperatures. (A) E_x at ϵ_{VHS} continues to soften with decreasing temperature as long as superconductivity is suppressed with a 2 T magnetic field (pink diamonds). In the presence of superconductivity, E_x hardens instead (0 T, red diamonds). The averaging window is a stress range of 0.05 GPa; the value of T_c is taken from (19). (B) E_x versus ϵ_{xx} at selected temperatures with and without an applied magnetic field (red, 0 T; pink, 2 T). The hardening is visible in the data at 1.9 K. The curves at 3 and 10 K have been offset by, respectively, 10 and 20 GPa for clarity. Data in (A) and (B) are from sample 3. (C) E_x versus temperature at ϵ_{VHS} (red), $0.4\epsilon_{VHS}$ (dark blue), and zero strain (light blue) over a wide range of temperatures. Open circles, sample 1; filled circles, sample 2. Data at ϵ_{VHS} for sample 2 are replotted from Fig. 2C. The averaging window is a strain range of 4.05×10^{-4} for sample 1 and 3×10^{-4} for sample 2.

A final aspect of our measurements is shown in Fig. 3C, in which we present E_x data over a wider range of temperatures, at zero strain, an intermediate strain, and the Van Hove strain. At zero strain, there is a broad minimum in the Young's modulus at $T \sim 40$ K, reflecting the fact that, unusually, Sr_2RuO_4 softens along the [100] crystalline direction as the temperature is decreased from room temperature (26). We show in fig. S8 that this feature is reproduced in our model, demonstrating that it too is a consequence of the conduction electrons in the γ sheet.

Discussion and outlook

Although the model that we have used to analyze our Sr_2RuO_4 data is specific to the Lifshitz transition in 2D, it can be viewed from a more general perspective that highlights the significance of low-temperature entanglement between electronic and elastic degrees of freedom and emphasizes the close connection between elastic response and entropy. Consider a quantum critical point (QCP) that can be crossed by varying some combination of elements of the strain tensor. Under the assumption that hyperscaling holds near any such a strain-tuned QCP, for the singular contribution to the entropy

$$S(T, \epsilon) = T^{d/z} \phi \left(\frac{\epsilon - \epsilon_c}{T^{1/\nu z}} \right) \quad (3)$$

where z and ν are the dynamical and correlation length exponents, respectively, d is the dimension of space, ϕ is a universal scaling function, and ϵ_c is the critical strain. The most notable consequence of Eq. 3 follows as one integrates the entropy with respect to temperature to obtain the free energy and then determine the elastic constant. Right at the QCP, where $|\epsilon - \epsilon_c|^{\nu z} \ll T$, it follows that

$$C = C_0 - \frac{\nu z}{\nu(d+z) - 2} \phi''(0) T^{\frac{\nu(d+z)}{\nu z} - 2} \quad (4)$$

where ϕ'' is the second derivative of ϕ . Here, C_0 is a temperature-independent background contribution to the elastic constant that enters as an integration constant for the free energy. Because the entropy is maximal at the QCP, $\phi'' < 0$. If $\nu(d+z) > 2$, then the universal temperature correction is small and positive and the system is mechanically stable. Conversely, the system must undergo an instability, defined by a vanishing elastic constant at a nonzero temperature, if the quantum Harris criterion $\nu(d+z) < 2$ (27, 28) is fulfilled. Then, the above scaling theory of a "naked" QCP ceases to be valid; the system either crosses over to a new critical regime where strain becomes a genuine dynamical quantum critical mode or undergoes a phase transition to another state of matter. As discussed in (22) and figs. S9 and S10, the Lifshitz point herein corresponds to $d = z = \nu^{-1} = 2$, placing us at the boundary of the

quantum Harris criterion, resulting in a logarithmic temperature dependence, and leading to a mechanical instability. If one takes the limit $v(d+z) \rightarrow 2$, appropriate for the 2D Lifshitz transition, then the exponent in the temperature-dependent term in Eq. 4 does not simply vanish because the prefactor $\frac{1}{v(d+z)^2}$ diverges at the same time. Instead, one recovers the logarithmic behavior of the Lifshitz transition.

Returning to the discussion of the experimental findings, the results presented herein constitute conclusive observation of a lattice softening driven by conduction electrons, the possibility of which was foreseen by Lifshitz >60 years ago (4). However, he considered hydrostatic pressure and transitions in materials with 3D electronic structure, in which case the relative change in bulk modulus would be $\sim 10^{-4}$, three orders of magnitude smaller than what we observed [(22) and figs. S11 and S12]. Partly for this reason, previous searches using hydrostatic pressure were unable to unambiguously resolve the predicted effect (29–33). Why, then, does it give such a prominent experimental signature in Sr_2RuO_4 ? First, we have worked with uniaxial rather than hydrostatic pressure. Also, Sr_2RuO_4 is an extremely clean material for which the relevant band is strongly 2D, preventing the logarithmic term in Eq. 2 from being washed out by 3D effects or disorder broadening. It is tempting on first inspection to assume that this logarithm makes the dominant contribution to the size of our signal, but for measurements performed at a few degrees kelvin, the size of the prefactor A actually plays the crucial role. It is hugely enhanced over Lifshitz’s original expectation for three reasons: (i) the correlation-induced γ band renormalization, (ii) the nonlinear Poisson’s ratio effect contribution to Young’s modulus, and (iii) the value of α in the deformation potential. In our model, the experimentally observed Van Hove strain yields $\alpha = 7.6$ and enters A as α^2 . To investigate further, we performed first-principles calculations, which emphasized that the γ band of Sr_2RuO_4 is based on Ru-O-Ru processes involving two d - p orbital hops, yielding $\alpha = 8$ [(22) and fig. S13].

Our findings also provide perspectives on the nature and consequences of the entanglement between elastic and electronic degrees of

freedom in metallic solids. To what extent might they be a driver for superconductivity as a route to avoid divergent lattice softening? Do the physics directly following from conduction electron density of states play a bigger than previously appreciated role in effects in heavy fermion physics such as the Kondo volume collapse (34) and lattice softening associated with magnetism (35) and metamagnetism (36)? Although these remain open questions, our observations provide strong and concrete evidence of relevance to the “chicken and egg” problem discussed in the introduction: Conduction band physics can drive unexpectedly large structural effects, and conduction electrons are not always slaves to the lattice.

REFERENCES AND NOTES

- E. Fradkin, S. A. Kivelson, M. J. Lawler, J. P. Eisenstein, A. P. Mackenzie, *Annu. Rev. Condens. Matter Phys.* **1**, 153–178 (2010).
- R. Fernandes, A. Chubukov, J. Schmalian, *Nat. Phys.* **10**, 97–104 (2014).
- J. H. Chu, H. H. Kuo, J. G. Analytis, I. R. Fisher, *Science* **337**, 710–712 (2012).
- I. M. Lifshitz, *Sov. Phys. JETP* **11**, 1130–1135 (1960).
- M. E. Barber, A. S. Gibbs, Y. Maeno, A. P. Mackenzie, C. W. Hicks, *Phys. Rev. Lett.* **120**, 076602 (2018).
- V. Sunko et al., *NPJ Quantum Mater.* **4**, 46 (2019).
- L. Van Hove, *Phys. Rev.* **89**, 1189–1193 (1953).
- A. P. Mackenzie, Y. Maeno, *Rev. Mod. Phys.* **75**, 657–712 (2003).
- Y. Maeno, S. Kittaka, T. Nomura, S. Yonezawa, K. Ishida, *J. Phys. Soc. Jpn.* **81**, 011009 (2012).
- C. Kallin, *Rep. Prog. Phys.* **75**, 042501 (2012).
- Y. Liu, Z. Q. Mao, *Physica C* **514**, 339–353 (2015).
- A. P. Mackenzie, T. Scaffidi, C. W. Hicks, Y. Maeno, *NPJ Quantum Mater.* **2**, 40 (2017).
- Y. Maeno et al., *J. Phys. Soc. Jpn.* **66**, 1405–1408 (1997).
- C. Bergemann, A. P. Mackenzie, S. R. Julian, D. Forsythe, E. Ohmichi, *Adv. Phys.* **52**, 639–725 (2003).
- J. S. Bobowski et al., *Condens. Matter* **4**, 6 (2019).
- K. M. Shen et al., *Phys. Rev. Lett.* **99**, 187001 (2007).
- A. Steppke et al., *Science* **355**, eaaf9398 (2017).
- M. E. Barber et al., *Phys. Rev. B* **100**, 245139 (2019).
- Y. S. Li et al., *Proc. Natl. Acad. Sci. U.S.A.* **118**, e2020492118 (2021).
- M. E. Barber, A. Steppke, A. P. Mackenzie, C. W. Hicks, *Rev. Sci. Instrum.* **90**, 023904 (2019).
- M. Ikhlas et al., *Appl. Phys. Lett.* **117**, 233502 (2020).
- See the supplementary materials.
- Y. S. Li et al., *Nature* **607**, 276–280 (2022).
- A. P. Mackenzie et al., *J. Phys. Soc. Jpn.* **67**, 385–388 (1998).
- B. Burganov et al., *Phys. Rev. Lett.* **116**, 197003 (2016).
- N. Okuda, T. Suzuki, Z. Mao, Y. Maeno, T. Fujita, *J. Phys. Soc. Jpn.* **71**, 1134–1139 (2002).
- M. Zacharias, A. Rosch, M. Garst, *Eur. Phys. J. Spec. Top.* **224**, 1021–1040 (2015).
- P. Chandra, P. Coleman, M. A. Continentino, G. G. Lonzarich, *Phys. Rev. Res.* **2**, 043440 (2020).
- L. Dubrovinsky et al., *Nature* **525**, 226–229 (2015).

- G. Steinle Neumann, L. Stixrude, R. E. Cohen, *Phys. Rev. B* **63**, 054103 (2001).
- G. Aquilanti et al., *Phys. Rev. B* **76**, 144102 (2007).
- B. K. Godwal, S. V. Raju, Z. Geballe, R. Jeanloz, *J. Phys. Conf. Ser.* **377**, 012033 (2012).
- Ya. M. Blanter, M. I. Kaganov, A. V. Pantsulaya, A. A. Varlamov, *Phys. Rep.* **245**, 159–257 (1994).
- J. W. Allen, R. M. Martin, *Phys. Rev. Lett.* **49**, 1106–1110 (1982).
- H. Rosner et al., *Nat. Phys.* **2**, 469–472 (2006).
- F. Weickert, M. Brandt, F. Steglich, P. Gegenwart, M. Garst, *Phys. Rev. B* **81**, 134438 (2010).
- Data for: H. M. L. Noad et al., Giant lattice softening at a Lifshitz transition in Sr_2RuO_4 , Edmond (2023); <https://doi.org/10.17617/3.UOVU60>.

ACKNOWLEDGMENTS

Funding: This work was supported by the Max Planck Society; Research in Dresden benefits from the environment provided by the DFG Cluster of Excellence (ct.qmat EXC 2147, Project 390858940 to A.P.M.); the German Research Foundation (TRR 288 422213477 ELASTO Q MAT, Project A10 to H.M.L.N., A.P.M., and C.W.H.; TRR 288 422213477 ELASTO Q MAT, Project A11 to M.G.; and TRR 288 422213477 ELASTO Q MAT, Project B01 to J.S. and V.S.); the Alexander von Humboldt Foundation (Research Fellowship for Postdoctoral Researchers to H.M.L.N.); received funding of the Klaus Tschira Boost Fund, a joint initiative of the German Scholars Organization and the Klaus Tschira Foundation (to H.M.L.N.); the Japan Society for the Promotion of Science (Overseas Research Fellowship to K.I. and KAKENHI Grants in Aid for Scientific Research grants 17H06136, 18K04715, 21H01033, and 22K19093 to N.K.; and Core to Core Program grant JPJSCCA20170002 to N.K.); the Japan Science and Technology Agency (JST) Mirai Program (grant no. JPMJMI18A3 to N.K.); and the National Research Foundation of Korea (grants 2021R1C1C1007017 and 2022M3H4A1A04074153 to B.K.). **Author contributions:** Conceptualization: H.M.L.N., J.S., C.W.H.; Formal analysis: H.M.L.N., M.G., J.S., C.W.H.; Funding acquisition: M.G., J.S., A.P.M., C.W.H.; Investigation: H.M.L.N., K.I., Y. S.L., E.G., V.S., B.K., I.I.M., M.G., J.S.; Methodology: H.M.L.N., E.G., V.S., J.S., C.W.H.; Project administration: H.M.L.N., A.P.M.; Resources: N.K., D.A.S.; Supervision: M.N., I.I.M., J.S., A.P.M., C.W.H.; Visualization: H.M.L.N.; Writing – original draft: H.M.L.N., M.G., J.S., B.K., I.I.M., A.P.M., C.W.H.; Writing – review and editing: H.M.L.N., K.I., Y. S.L., N.K., M.N., B.K., I.I.M., M.G., J.S., A.P.M., C.W.H. **Competing interests:** C.W.H. has 31% ownership of Razorbill Instruments, a company that markets uniaxial pressure cells. C.W.H. is a coapplicant on patent application GB1711384.6, which relates to the methodology in this work. The remaining authors declare no competing interests. **Data and materials availability:** Data in the main text and supplementary materials are available at Edmond, the open research data repository of the Max Planck Society (37).